Transport and trapping of photocharges in liquid crystals placed between photoconductive polymer layers

Junho Mun, Choon Sup Yoon, Hyun-Wuk Kim, Su-An Choi, and Jong-Duk Kim

Additional information on Appl. Phys. Lett.

Transport and trapping of photocharges in liquid crystals placed between photoconductive polymer layers

Junho Mun and Choon Sup Yoon[a)]
Department of Physics, KAIST, Daeduck Science Town, Taejon 305-701, Korea

Hyun-Wuk Kim, Su-An Choi, and Jong-Duk Kim
Department of Chemical Engineering, KAIST, Daeduck Science Town, Taejon 305-701, Korea

The transport and trapping of photocharges in liquid crystals placed between photoconductive polymer layers was investigated systematically. The transport of the photocharges is explained in terms of current paths that are formed along the bright sites of an interference pattern. Our study shows clearly that charge trapping occurs predominantly in the photoconductive poly(N-vinylcarbazole) layers and not in the insulating poly(vinyl alcohol) layers, contrary to a previous report. © *2001 American Institute of Physics.* [DOI: 10.1063/1.1400087]

Photorefractive (PR) effects in nematic liquid crystals attract much interest because of the extremely large change of refractive index that can be induced in them by lasers. Liquid crystals require neither nonlinear optical chromophores nor the application of a high voltage of several kV for the formation of diffraction gratings, unlike electrooptically induced photorefractive polymers.[1] PR effects in pure liquid crystals,[2] charge generator doped liquid crystals,[3,4] monomer doped liquid crystals,[5,6] nonlinear optical polymer dispersed liquid crystals,[7,8] and liquid crystals placed between photoconductive polymer layers (LCPPL),[9–11] have been reported. The PR effect in LCPPL was first studied by Ono and Kawatsuki,[9,10] who reported that the diffraction efficiency in LCPPL vanished at steady state where a nematic liquid-crystal layer was placed between photoconductive poly(N-vinylcarbazole) (PVK) layers doped with charge generators.[9] We, by contrast, observed a significant diffraction efficiency in LCPPL of the same structure. The rather surprising discrepancy between Ono's results and ours necessitates a systematic study to verify the formation of diffraction gratings in LCPPL.

Figure 1 shows the basic structure of the samples used in this study, which consists of the following layers, in order: an indium–tin–oxide (ITO) glass electrode, poly(vinyl alcohol) (PVA), PVK, E7 liquid crystal, PVK, PVA, and an ITO glass electrode (sample 2 in Table I). PVA was used as an insulator and PVK as a charge-trapping medium. The E7 nematic liquid crystal was purchased from Merck Ltd. Fullerene (C_{60}) was used as a charge generator and its concentration in both the PVK and liquid-crystal layers was 0.05 wt %.

The composition of nine different samples that consisted of various combinations of PVK and PVA layers and an E7 liquid-crystal layer are listed in Table I. The PVK and PVA layers were spin coated and the thickness of the layers was about 1 μm. The thickness of the liquid-crystal layer was maintained by a spacer of 12 μm.

A linearly polarized single-mode He–Ne laser of 17 mW (Melles-Griot, 05LHP925) was used for two-beam coupling

and diffraction efficiency measurements. The intensity of two p-polarized writing beams was 350 mW/cm^2 and the angle between the beams was 0.026 rad. The sample normal was tilted by 30° from the acute angle bisector of the two beams. Figure 2 shows a typical asymmetric two-beam coupling in a C_{60} doped E7 liquid-crystal layer placed between two C_{60} doped PVK layers (sample 8 in Table I), which confirms a nonlocal PR effect.

The PR effect in LCPPL was investigated by measuring the first-order Raman–Nath diffraction efficiency. The steady-state diffraction efficiency, grating formation time, coupling ratio, and gain coefficient of the nine samples are also summarized in Table I. The maximum diffraction efficiency in liquid-crystal systems is a function of the voltage applied, because of the molecular reorientational photorefractive effect.[12] Figure 3 illustrates that a film consisting of PVK–C_{60}/E7–C_{60}/PVK–C_{60} layers (sample 8) behaves in the manner just mentioned. The maximum diffraction efficiency values are given in the fourth column from the right of Table I and the applied voltages that yielded them are given in parentheses. If insulating layers (PVA) are placed between the PVK and E7 layers, the voltage that gives the maximum diffraction efficiency increases to above 100 V, which is the threshold for obtaining stable diffraction signals. Therefore, it should be noted that the voltages presented for samples 7 and 9 of Table I are not the values for producing the maximum diffraction efficiency, but the maximum that may be applied while maintaining stability.

When two coherent beams were incident on the same spot of a sample, an interference pattern was formed and photocharges were generated at the bright sites if the sample contained charge generators. The generated photocharges acted as charge carriers and the conductivity was much
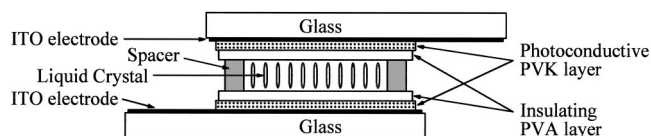

FIG. 1. Basic structure of photorefractive liquid-crystal samples, which corresponds to sample 2 in Table I.

[a)]Electronic mail: csyoon@mail.kaist.ac.kr

TABLE I. Diffraction efficiency, grating formation time, coupling ratio, and gain coefficient of LCPPL samples of various compositions.

	Constitution								
Sample	Upper charge trapping layer	Upper insulating layer	Liquid crystal	Lower insulating layer	Lower charge trapping layer	Diffraction efficiency (%)	Grating formation time (ms)	Coupling ratio (γ)	Gain coefficient (cm^{-1})
1	PVK[a]		E7[b]		PVK	0			
2	PVK	PVA[c]	E7	PVA	PVK	0			
3			E7–C_{60}			0.24 (4 V)	365	1.062	89
4	PVK		E7–C_{60}		PVK	2.6 (40 V)	156	1.212	310
5	PVK	PVA	E7–C_{60}	PVA	PVK	~0			
6	PVK–C_{60}		E7		PVK–C_{30}	2.0 (40 V)	278	1.144	210
7	PVK–C_{60}	PVA	E7	PVA	PVK–C_{60}	0.69 (100 V)	68	1.065	94
8	PVK–C_{60}		E7–C_{60}		PVK–C_{60}	3.7 (8 V)	187	1.151	220
9	PVK–C_{60}	PVA	E7–C_{60}	PVA	PVA–C_{60}	1.2 (100 V)	274	...[d]	...[d]

[a]PVK: poly(*N*-vinylcarbazole).
[b]E7: liquid crystal (Merck Co.).
[c]PVA: poly(vinyl alcohol).
[d]Could not be measured because of severe energy loss of the two incident beams to the higher-order diffraction.

higher at the bright sites than at the dark ones. Current paths were then formed along the bright sites across the sample when an external dc voltage was applied. In the case of sample 8, a photocurrent of 76 nA/cm² was observed when two writing beams of 350 mW/cm² were incident on a sample while applying a voltage of 8 V.

Samples 1 and 2, which were not doped with fullerene in the PVK, PVA, and E7 layers, showed no diffraction efficiency at all, which clearly indicates that there was no PR effect.

A lone E7 liquid-crystal layer doped with fullerene (sample 3) showed a diffraction efficiency of 0.24%. However, the diffraction efficiency could be enhanced more than tenfold simply by placing PVK layers on both sides of the E7–C_{60} layer (sample 4). When dc voltage was applied, the charges generated from the fullerene molecules of the E7 layer were transported to the PVK layers along the current paths across the sample. Then, the charges moved to the sides of the bright sites in the PVK layers by diffusion and drift, and were trapped by defects so that a space-charge distribution and, in consequence, a space-charge field could be established in the PVK layers. The penetration field of the space-charge field in the PVK layers into the E7 liquid-crystal layer caused the liquid-crystal molecules to reorient along the field, which resulted in changes of the refractive index. Since the space-charge field was out of phase with the space-charge distribution, the refractive-index grating and the interference pattern became out of phase and nonlocal PR effects occurred. When insulating PVA layers were introduced between the fullerene doped E7 layer and the PVK layers (sample 5), transportation of photocharges generated in the E7 layer to the PVK layers was blocked by the PVA layers. Therefore, the photocharges could not be injected effectively into the PVK layers and current paths were not formed along the bright sites. Since the PVK layer could not itself generate sufficient photocharges to form diffraction gratings, the diffraction efficiency in sample 5 almost vanished. From the results of samples 4 and 5, it is clear that the formation of current paths played an important role in generating PR gratings in sample 4, where only the liquid-crystal layer was doped with fullerene.

When the PVK layers of sample 1 were doped with fullerene (sample 6), photocharges generated at the bright sites of the PVK layers were transported to the sides by
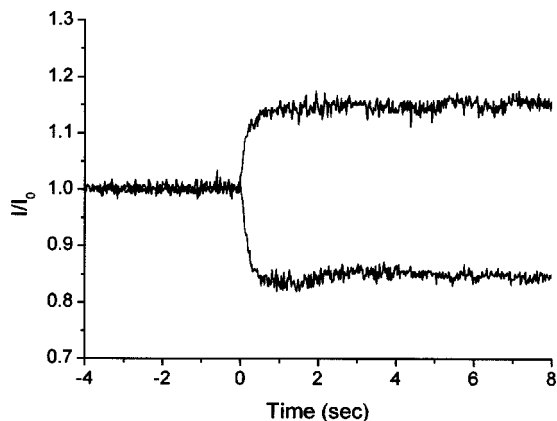

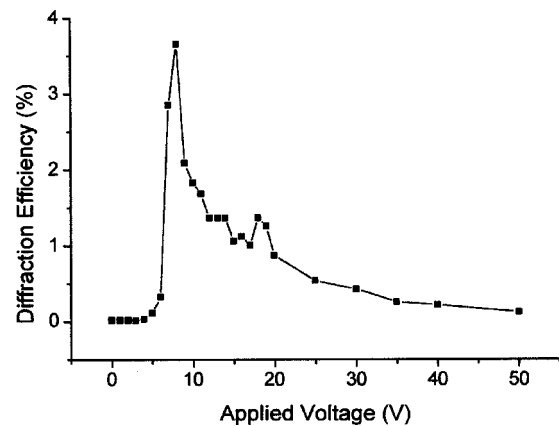FIG. 2. Energy exchange between two writing beams in sample 8.

FIG. 3. First-order Raman–Nath diffraction efficiency of PVK–C_{60}/E7–C_{60}/PVK–C_{60} layers (sample 8) as a function of applied voltage.

Appl. Phys. Lett., Vol. 79, No. 13, 24 September 2001

Mun *et al.* 1935
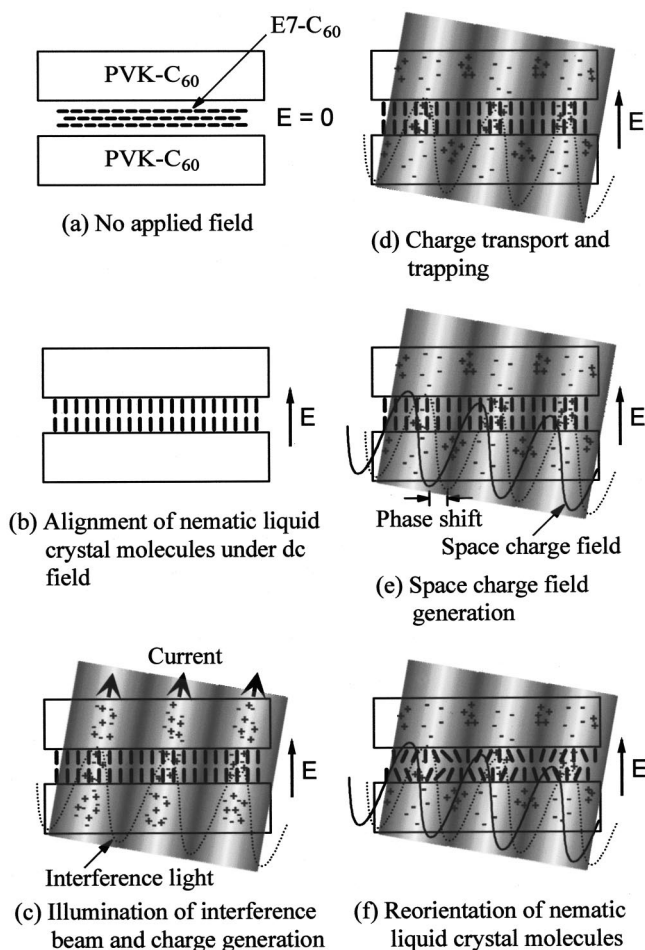
FIG. 4. Schematic illustration of current paths and photorefractive grating formation in PVK–C_{60}/E7–C_{60}/PVK–C_{60} layers (sample 8).

diffusion and drift, and were trapped in the same PVK layers to generate PR gratings. Although current paths were formed across the sample while an external field was applied, the current paths were not essential for producing PR gratings in this case because the photocharges generated in the PVK layers contributed to the formation of diffraction gratings in the same layers.

When insulating PVA layers were inserted between the E7 layer and the fullerene doped PVK layers of sample 6 (sample 7), current paths were not formed, as in the case of sample 5. The diffraction efficiency rose to about 3% at the beginning, decreased rapidly within seconds and gradually reached steady state in several minutes. The steady-state value is quoted in Table I. We attribute the rapid decrease of the diffraction signal to a drift of the space charges generated in the PVK–C_{60} layers to the interface between the bottom PVK–C_{60} layer and the neighboring PVA layer, and the interface between the top PVK–C_{60} layer and the neighboring ITO electrode. We ascribe the gradual decrease of the diffraction signal to a diffusion of the space charges that were piled up at the interfaces.

Ono and Kawatsuki studied a similar liquid-crystal (E44) system which had the same layer structure as sample 7 but used a different charge generator (2,4,7-trinitro-9-fluorenone). They observed a diffraction efficiency very similar to that of sample 7, but interpreted the PVA layers as charge trapping layers. However, while Ono and Kawatsuki[9]

observed no diffraction efficiency in samples that consist of a PVK-charge generator layer/E44 nematic liquid-crystal layer/PVK-charge generator layer, we observed a significant diffraction efficiency of 2.0% in sample 6. Our results show that the PVK layers trap dominant charges, as in sample 6. On the other hand, the PVA layers do not trap charges, because the introduction of the PVA layers between the PVK and E7–C_{60} layers into sample 4 resulted in the diffraction efficiency vanishing in sample 5.

The largest diffraction efficiency was obtained when both the E7 layer and the PVK layers of sample 1 were doped with fullerene (sample 8). Figure 4 shows a PR grating formation in sample 8. The charges generated at bright sites of the fullerene doped liquid-crystal layer moved to the top PVK layer along current paths [Fig. 4(c)]. Together with these charges, those generated at bright sites of the PVK layers diffused and drifted to the sides, and were trapped by defects in the PVK layers [Fig. 4(d)]. Both the charges generated from the liquid-crystal layer and the PVK layers contributed to the formation of a space-charge field [Fig. 4(e)]. Penetration of the space-charge field into the E7 liquid-crystal layer caused the liquid-crystal molecules to reorient [Fig. 4(f)] and this led to a large refractive-index change, which is demonstrated by the largest diffraction efficiency value of 3.7%.

The diffraction efficiency of sample 9 was reduced to 1.2% at 100 V when PVA insulating layers were introduced between the E7–C_{60} layer and the PVK–C_{60} layers of sample 8. Since the PVA insulating layers did not allow the charges generated in the E7–C_{60} liquid-crystal layer to be transported to the PVK–C_{60} layer, the charges generated in the PVK layers and the E7 layer contributed independently to the formation of a space-charge field. Again, the penetration field of the space-charge field into the E7–C_{60} layer was weakened by the presence of the PVA insulating layers. Consequently, the diffraction efficiency of sample 9 was reduced to about one third of that of sample 8.

In summary, the transport of photocharges in the LCPPL is explained by current paths that are formed along the bright sites of the interference pattern. Our study shows that the photoconductive PVK layers act as dominant charge trapping layers in LCPPL systems while the insulating PVA layers do not.

[1] W. E. Moerner, A. Grunnet-Jepsen, and C. L. Thompson, Annu. Rev. Mater. Sci. **27**, 585 (1997).
[2] I. C. Khoo, H. Li, and Y. Liang, Opt. Lett. **19**, 1723 (1994).
[3] E. V. Rudenko and A. V. Sukhov, JETP Lett. **59**, 142 (1994).
[4] H. Ono, I. Saito, and N. Kawatsuki, Appl. Phys. Lett. **72**, 1942 (1998).
[5] G. P. Wiederrecht, B. A. Yoon, and M. R. Wasielewski, Science **270**, 1794 (1995).
[6] G. P. Wiederrecht, M. P. Niemczyk, W. A. Svec, and M. R. Wasielewski, Chem. Mater. **11**, 1409 (1999).
[7] A. Golemme, B. L. Volodin, B. Kippelen, and N. Peyghambarian, Opt. Lett. **22**, 1226 (1997).
[8] G. Cipparrone, A. Mazzulla, and F. Simoni, Opt. Lett. **23**, 1505 (1998).
[9] H. Ono and N. Kawatsuki, Appl. Phys. Lett. **71**, 1162 (1997).
[10] H. Ono and N. Kawatsuki, Opt. Commun. **147**, 237 (1998).
[11] A. Miniewicz, S. Bartkiewicz, A. Januszko, and J. Parka, J. Inclusion Phenom. Macrocylic Chem. **35**, 317 (1999).
[12] S. Bartkiewicz and A. Miniewicz, Adv. Mater. Opt. Electron. **6**, 219 (1996).